JOURNAL OF MATERIALS SCIENCE 16 (1981) 1477–1489

Microstructural characterization of calcium flouride single crystals deformed in steady state

WILLIAM M. SHERRY*, JOHN B. VANDER SANDE
Department of Materials Science and Engineering, Massachusetts Institute of Technology, Cambridge, Massachusetts 02139, USA

Calcium fluoride single crystals have been deformed in compression to conditions of steady-state deformation in the temperature range 590 to 907° C (0.53 to 0.72 T/T_m). The deformation microstructures have been characterized using cold-stage transmission electron microscopy. The microstructure of deformed samples is seen to consist of dislocation tangles, networks and subgrain boundaries. Dislocation structures in the subgrain boundaries have been characterized and the effect of the temperature of deformation on the subgrain boundary structure has been established. The flow stress, σ, during steady-state deformation, has been found to be proportional to $d^{-1.14}$, where d is the subgrain size. The steady-state deformation behaviour is believed to be controlled by the mechanisms of obstacle-limited glide of dislocations and power-law creep. During characterization of the deformation microstructures, regions of non-uniform cell or subgrain boundary structure have been observed. It has been suggested that such regions arise from either non-uniform deformation or recovery and recrystallization. Despite the presence of such regions, subgrain strengthening appears to be a viable means of improving the flow stress of calcium fluoride single crystals.

1. Introduction

The advent of high-power laser systems has stimulated interest in the fabrication of alkali halide and alkaline-earth halide materials which can function as windows or lenses and also possess sufficient mechanical strength to provide in-service stability under mechanical and thermal induced loading. Increases in the yield strength of metals, e.g. iron [1], copper [2–4], silver [5], copper–aluminum [6], and aluminum [7] have been achieved solely through mechanical deformation, resulting in a microstructure composed of dislocation cells or subgrains. Deformation experiments on pure and doped KCl [8–10], single and polycrystalline NaCl [9] and pure and Mg-doped LiF [11] have achieved substantial strength improvements through subgrain formation. The predicted inverse relationship between flow stress, σ, and subgrain size, d, has been verified [1, 4, 12] in both classes of materials, thus demonstrating the important influence of cell or subgrain size on the mechanical strength.

The potential of subgrain strengthening in the alkali and alkaline-earth halides has led to a number of investigations of substructure development during hot forging. The microstructure produced in hot-forged single crystal calcium fluoride has been followed using light microscopy and has been shown to depend directly on stress and strain and indirectly on temperature [13]. High-temperature deformation of single-crystal alkaline-earth halides [14–16] may introduce a fine-grained microstructure that provides increases of the yield stress and fracture stress with little loss of the optical properties. Isostatic forging below the recrystallization temperature has produced crack-

* Present address: Bell Laboratories, 555 Union Boulevard, Allentown, Pennsylvania 18103, USA.

0022–2461/81/061477–13$03.30/0

TABLE I Temperatures, stresses, and strains of hot-forged calcium fluoride

Temperature (°C)	Stress (MPa)	True strain
590	36.54	0.30
702	27.57	0.45
795	22.75	0.45
817	–	0.45
907	17.65	0.50

free, fine-grained material from calcium fluoride single crystals and increases in the fracture energy, γ_c, thus reducing the tendency for calcium fluoride to cleave catastrophically in {1 1 1} type planes [17]. However, residual stresses in calcium fluoride forged at these lower temperatures may degrade the optical performance. Stress-relief annealing of forged samples removes the strain and usually results in a coarse-grain microstructure along with losses in the additional strength gained through deformation. Hot forging at even higher temperatures produces larger, and more varied, subgrain sizes (0.5 to 4 mm) with smaller increases in the yield stress. Furthermore, at these higher forging temperatures, recrystallization may occur.

In the following, the microstructures developed during steady-state deformation of calcium fluoride in the temperature range 0.53 to $0.72\,T/T_m$ (590 to 907°C), where T is the temperature and T_m is the melting-point temperature, are investigated using transmission electron microscopy (TEM). The relationship between macroscopic flow stress and subgrain size is established and the importance of deformation temperature on the recovery of deformation microstructures is assessed.

2. Experimental technique

Calcium fluoride single crystals of random orientation were purchased from Harshaw Chemical Co. for the compressive deformation experiments. Samples, in the form of right circular cylinders with an initial height to diamater ratio of 1:1, were compressed at an initial strain rate of $4.0 \times 10^{-2}\,\text{sec}^{-1}$ (see Table I for a schedule of forging temperatures, stresses and strains). At the end of deformation, specimens were immediately removed from the hot press and allowed to cool to room temperature. Grafoil was used as a lubricant to reduce the frictional forces between the deformation plattens and the ends of the samples.

True stress–true strain curves were calculated after correcting the compression data for frictional forces between the plattens and sample [18], using

$$\sigma_y = \frac{P}{\left(1 + \frac{\mu}{3}\frac{D}{H}\right)}, \quad (1)$$

where σ_y is the flow stress, P is the average forging pressure, μ is the coefficient of friction, and D/H is the diameter to height ratio of the specimen.

Transmission electron microscopy of the deformation microstructure was performed using a Philips EM300 transmission electron microscope. Due to ionization radiation damage caused by the electron beam, a double-tilt liquid-helium cold-stage was used to minimize the rate of agglomeration of defects. Details of the ionization radiation damage process and the advantages accrued by low-temperature microscopy have been previously described [19].

TEM specimens were prepared by chemically thinning calcium fluoride in a Fischione dual jet polisher. Thinning was acomplished using a solution of 425 ml H_2O, 75 ml HCl, 50 g $AlCl_3$ and 50 g NH_4Cl at a temperature of 70° C. All TEM samples were coated with a layer of evaporated carbon to prevent charging. Samples were secured in the helium stage at one point with silver paint to provide thermal and electrical conduction and to allow the sample to contract freely during the cooling procedure. Cooling rates were restricted to a maximum of $2\,\text{K}\,\text{sec}^{-1}$ to prevent the introduction of dislocations by thermal stress. Conventional [20] **g.b** experiments were performed to determine the nature of the Burgers vectors, **b**, in the dislocation structures (**g** is the diffracting vector). Subgrain sizes and dislocation densities were calculated using standard quantitative metallographic techniques [21].

3. Results

Characterization of the microstructure of hot-forged calcium fluoride was performed considering the structure of the subgrain boundaries produced by deformation, the relationship between the subgrain size and macroscopic flow stress, and the effect of temperature on the development and stabilization of a steady-state deformation microstructure.

3.1. Subgrain boundary structure

3.1.1. Dislocation structure of the subgrain boundaries

A condition of steady-state deformation was achieved for all samples forged in the temperature range 0.53 to $0.72\,T/T_m$. The nature of the sub-

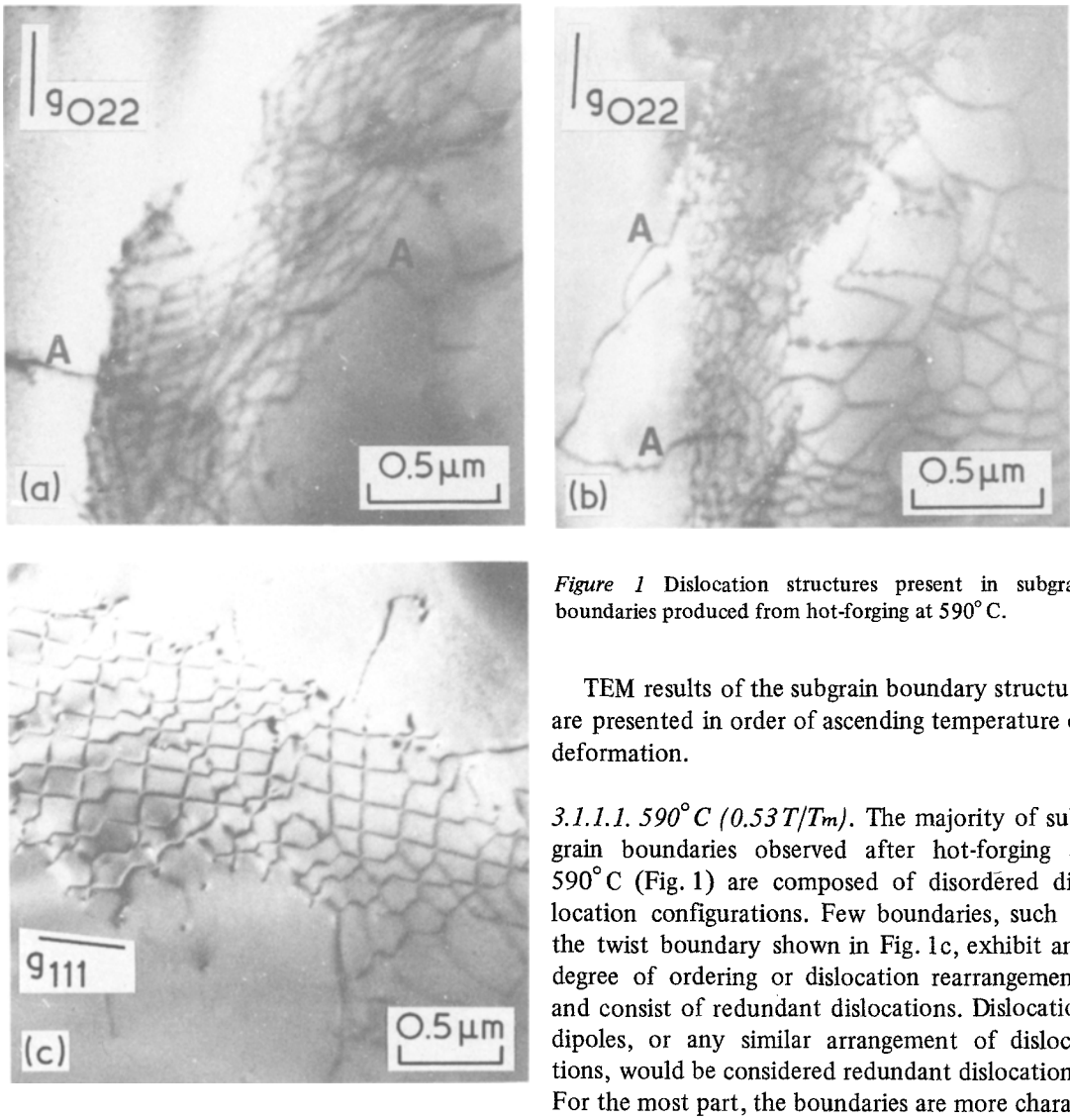

Figure 1 Dislocation structures present in subgrain boundaries produced from hot-forging at 590° C.

grain boundary structure was found to be indirectly dependent on temperature while the subgrain size and structure of the boundary was directly dependent on stress. The subgrain boundary structure was interpreted based on two types of defects which comprise the boundary. These are:

(1) Intrinsic subgrain boundary dislocations which are a requirement of the boundary geometry and are associated with equilibrium subgrain boundaries.

(2) Extrinsic subgrain boundary dislocations which are those dislocations resulting from the accommodation of lattice dislocations into the boundary and are not a requirement of boundary geometry but decrease the energy of the system while increasing the energy of the boundary.

TEM results of the subgrain boundary structure are presented in order of ascending temperature of deformation.

3.1.1.1. 590° C (0.53 T/T_m). The majority of subgrain boundaries observed after hot-forging at 590° C (Fig. 1) are composed of disordered dislocation configurations. Few boundaries, such as the twist boundary shown in Fig. 1c, exhibit any degree of ordering or dislocation rearrangement, and consist of redundant dislocations. Dislocation dipoles, or any similar arrangement of dislocations, would be considered redundant dislocations. For the most part, the boundaries are more characteristic of cell walls produced by deformation at temperatures below half the absolute melting temperature [19]. Evidence for the interaction of matrix dislocations (see dislocations labeled A in Fig. 1a and b) with the boundary is observed, while in these micrographs no evidence is given for the accommodation of these dislocations into the boundaries. The non-equilibrium nature of the boundaries suggests that little rearrangement of the structure has occurred through thermally-assisted recovery processes.

3.1.1.2. 702° C (0.60 T/T_m). Increasing the temperature of hot-forging to 702° C produces subgrain boundaries with a higher degree of order (see Fig. 2). The boundary structure has an increased degree of periodicity, as exemplified by the tilt

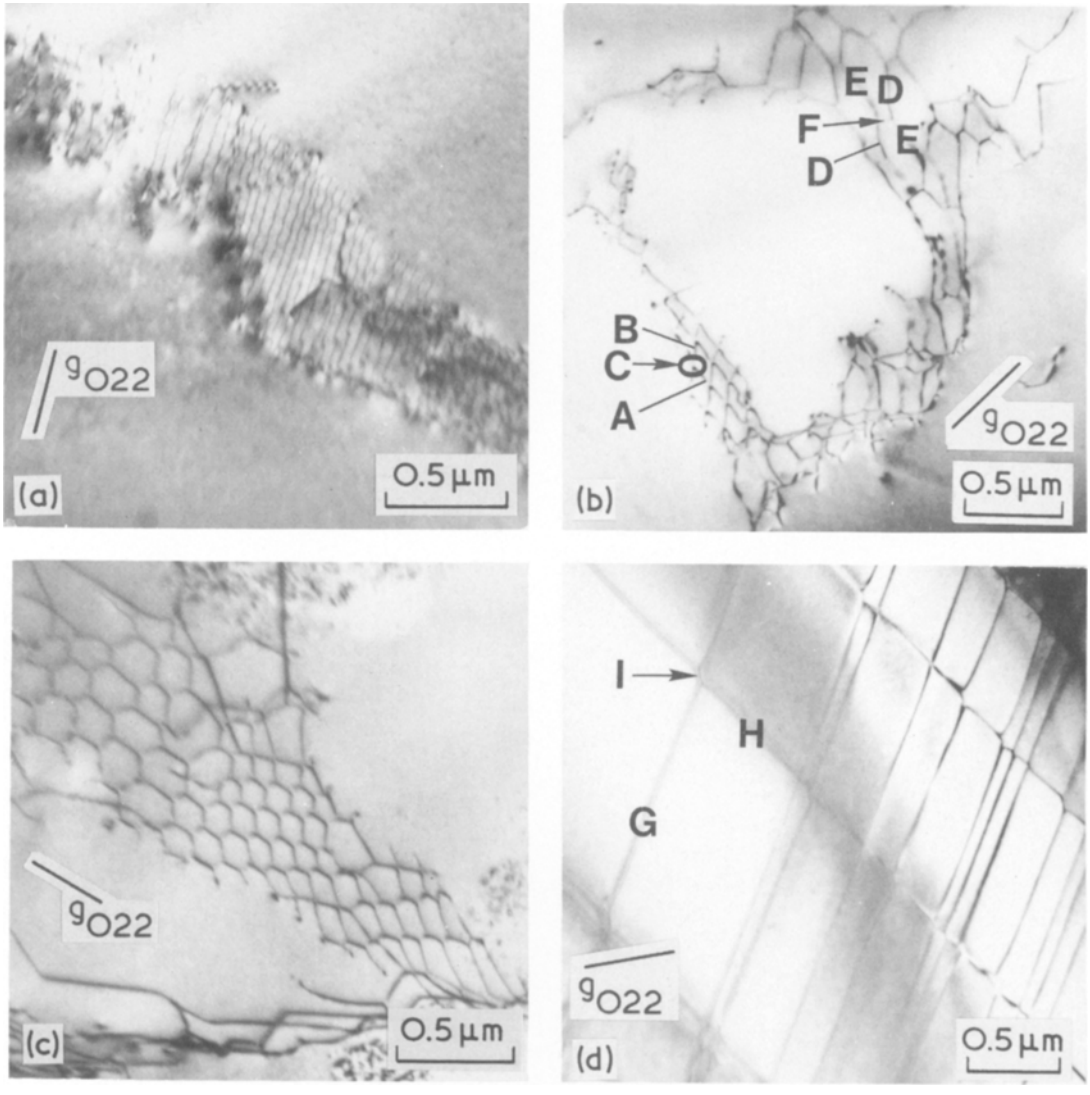

Figure 2 Subgrain boundary structures observed in samples hot-forged at 702° C. Note the knitting of dislocations into more regular networks.

boundary of Fig. 2a and the twist boundary of Fig. 2c, and fewer boundaries consist of random dislocation tangles.

The intrinsic dislocations of the simple tilt boundary presented in Fig. 2a are easily discerned by their narrow image widths. Extrinsic dislocations present in the boundary can be seen directly and by the discontinuities these dislocations cause in the intrinsic dislocations (the extrinsic dislocations may be seen by using other Bragg reflections). The angular misorientation produced by the tilt boundary in Fig. 2a was determined to be 0.36° by measuring the relative displacement of Kikuchi lines in the electron diffraction patterns of the adjoining subgrains. Assuming the boundary in Fig. 2a is a simple tilt boundary with an average dislocation spacing of 50 nm, the calculated boundary misorientation is 0.46°.

The nature of the Burgers vectors of the dislocations comprising subgrain boundaries A–B–C and D–E–F of Fig. 2b were established. The reactions which occur are

$$\mathrm{A} + \mathrm{B} = \mathrm{C} \quad \frac{a}{2}[10\bar{1}] + \frac{a}{2}[101] \rightarrow a[100] \qquad (2)$$

and

$$\mathrm{E} + \mathrm{F} = \mathrm{D} \quad \frac{a}{2}[10\bar{1}] + \frac{a}{2}[011] \rightarrow \frac{a}{2}[110], \qquad (3)$$

where a is the lattice parameter. The energy requirements of Equations 2 and 3 may be calculated assuming the elastic strain energy is proportional to $\mathbf{b}^2$, where $\mathbf{b}$ is the Burgers vector of a dislocation. Equation 3 is clearly favourable while the energies of reactants and products of Equation 2 are equal. The Burgers vectors of dislocations A and B are inclined by approximately 45° and 30° to their respective dislocation lines, while that of dislocation C is nearly parallel. Thus dislocations A and B are mixed in character, and C is almost pure screw. Since the energy of edge dislocations $[\alpha b^2/(1-\nu)]$ is greater than that of screw dislocations (αb^2), in any reaction such as Equation 2, where the reactants have a significant edge component and the product is primarily screw in nature, the reaction is favourable [22].

An array of dislocations arranged nearly parallel to the surface of the foil is presented in Fig. 2d. Dislocations G and H may be attractive and produce the following reaction:

$$G + H = I \quad \frac{a}{2}[01\bar{1}] + \frac{a}{2}[101] \rightarrow \frac{a}{2}[110]. \quad (4)$$

Both dislocations G and H are almost pure edge in character, and dislocation I is also pure edge. Several of the G-type dislocations must be dipoles since one of the two adjacent G-type dislocations reacts with an H dislocation, while the second produces no reaction.

3.1.1.3. 817° C ($0.67 T/T_m$). Subgrain boundaries characteristic of those produced from hot forging at 817° C are presented in Fig. 3. The degree of ordering within the boundaries has increased over that of boundaries produced at lower forging temperatures. Boundary dislocations occur at shorter periodic intervals and are primarily intrinsic in nature. Many of the boundaries are not curved locally, thus the dislocation structure and energy of the subgrain boundary are constant in these regions. An exception is seen in Fig. 3a where a portion of the boundary is seen to bow out, and, associated with this, the dislocation structure changes along the bowed-out segment. A triple point, shown in Fig. 3b, is formed by the intersection of two highly ordered twist-type boundaries consisting of diamond-shaped dislocation cells. The junction formed by two tilt boundaries is shown in Fig. 3c, while a compound twist–tilt boundary composed of a regular array of hexagonal-shaped cells characteristic of the twist portion superimposed on an array of parallel dislocations characteristic of the tilt portion is presented in Fig. 3d.

TABLE II Average subgrain boundary angles

Temperature (° C)	Angle (degrees)	Standard deviation (degrees)
590	1.06	0.35
702	1.51	1.44
817	1.21	0.75
907	0.99	0.35

3.1.1.4. 907° C ($0.72 T/T_m$). Hot forging at 907° C produces a microstructure composed of highly ordered subgrain boundaries, where the boundary dislocation structure is periodic over short distances (see Fig. 4). Most boundaries are composed almost exclusively of intrinsic dislocations. The density of extrinsic dislocations is very low, suggesting that these dislocations may have been annihilated by interactions within the subgrains or accommodated into the subgrain boundary structure. A subgrain boundary, with a highly periodic structure, and boundary defect (labeled A) are shown in Fig. 4b. These defects may be ledges produced by the intersection of extrinsic dislocations with the boundary or a result of misorientation changes in the boundary. The apparent migration of extrinsic dislocations (labelled B and C) to a subgrain boundary is shown in Fig. 4c. It is possible that these dislocations are being accommodated into the boundary as a mechanism in the overall recrystallization or deformation process.

3.1.2. Misorientation angles of the subgrain boundaries

Misorientation angles of the subgrain boundaries were determined using two different TEM diffraction techniques. The splitting of electron diffraction spots and the shift in Kikuchi lines produced by subgrain to subgrain misorientation were measured. Table II presents a summary of the average subgrain angles measured as a function of forging temperature. The standard derivation of the measurements is also included in Table II. With few exceptions the subgrain boundary angles were less than 2.0° in misorientation. No obvious correlation exists between the measured subgrain boundary angles and the forging temperature or flow stress.

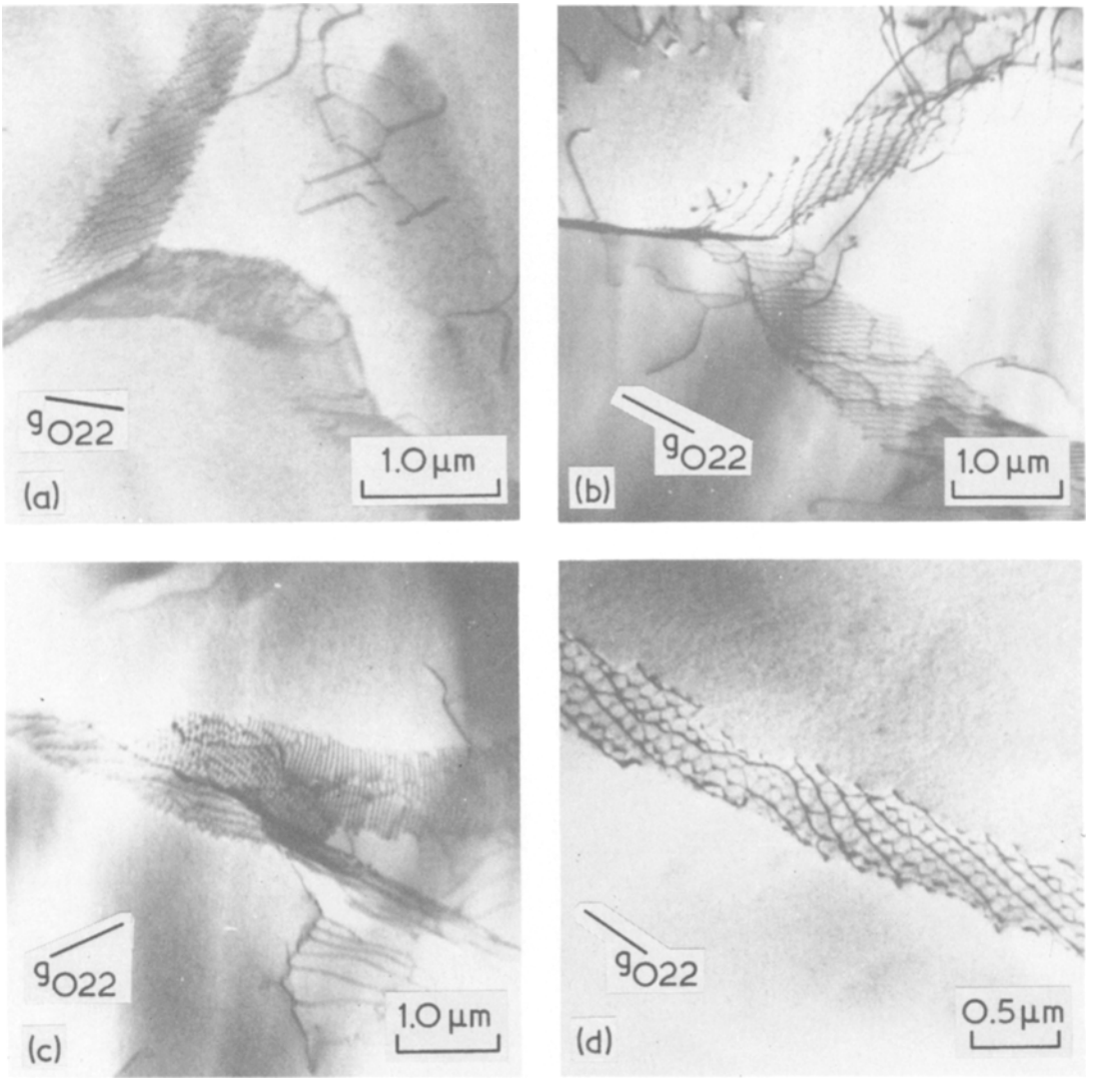

Figure 3 Micrographs of the subgrain boundaries observed in samples hot-forged at 817° C. The boundaries display a higher degree of periodicity over those present in samples forged at lower temperatures.

3.2. Subgrain size–flow stress relationship

A composite TEM micrograph of the subgrain morphology of a sample hot-forged at 590° C, and typical of those used to determine the size of subgrains developed from hot forging at 590, 702, 795 and 907° C is presented in Fig. 5. The subgrain boundaries are well developed, with a uniform subgrain size. A compilation of the sub-grain sizes measured from TEM micrographs of samples forged at 590, 702, 795 and 970° C is shown in Fig. 6 in the form of a plot of log flow stress against log subgrain size. A least-squares fit regression analysis of the data plotted in Fig. 6 yields the power-law dependence

$$\sigma = 4.378 G \mathbf{b} d^{-1.14} , \quad (5)$$

where it is seen the flow stress, σ (kg mm^{-2}) is approximately inversely proportional to the subgrain size, d(mm). G is the shear modulus (kg mm^{-2}).

3.3. Non-uniform hot-forged microstructures

In addition to the well-developed subgrain microstructures seen in Fig. 5, a region was observed in a sample hot-forged at 590° C (Fig. 7) consisting of a duplex subgrain microstructure. Within the more developed, densely dislocated boundaries of Fig. 7

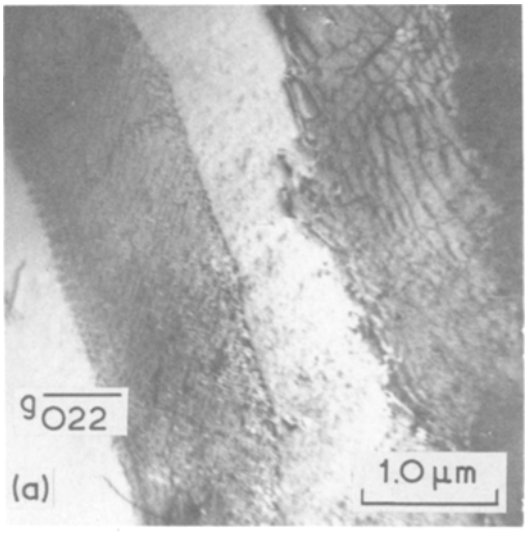

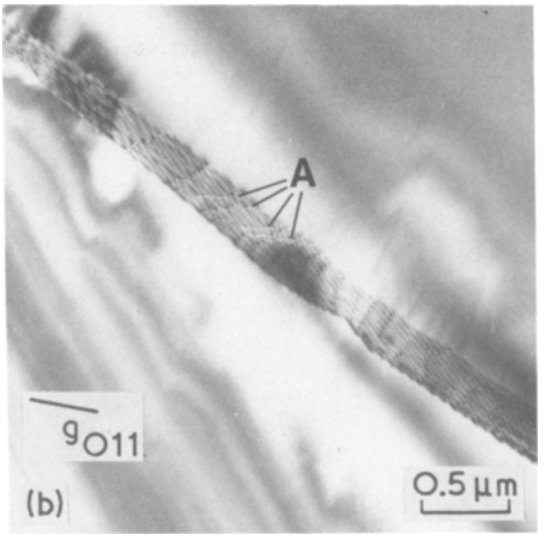

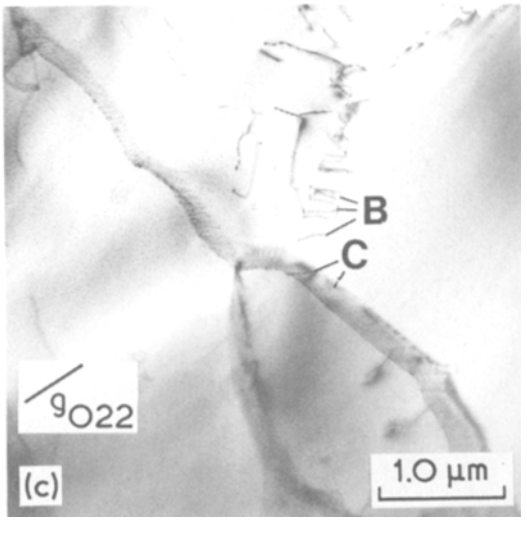

Figure 4 Subgrain boundaries produced from hot-forging at 907° C. At this temperature, boundaries exhibited the highest degree of order.

are several lower density boundaries. The larger, denser boundary has dimensions of approximately 20 to 30 μm, while the less dense boundaries are 4 to 6 μm in size. The less dense boundaries are similar to cell walls or dislocation tangles as opposed to subgrain boundaries. Since these boundaries are not well developed, it appears that they are in the process of developing or annihilating. At an even higher temperature of 907° C (Fig. 8), where thermal activation of diffusional recovery processes of the dislocation structures may play a more important role during hot forging, an area was observed consisting of dislocation tangles with no resemblance to a subgrain structure. This type of microstructure suggests that some form of recrystallization or subgrain migration may have occurred, the nature of which will be considered in a later section.

4. Discussion

The steady-state deformation microstructure of calcium fluoride single crystals hot forged at temperatures of 590, 702, 795, 817 and 907° C has been shown to consist of a network of subgrains and/or dislocation cells. A range of subgrain boundary structures was observed depending on the temperature of deformation. At the lower temperatures of deformation, the microstructure contained both subgrain and cell-wall boundaries. The cell-wall-type boundaries were, in general, disordered and contained many redundant dislocations, e.g. dipoles. In such boundaries the distinction between intrinsic and extrinsic dislocations is at best difficult since the boundary plane is not well defined. At higher temperatures only subgrain boundaries are observed. The structure in the subgrain boundaries is highly periodic (ordered), consisting for the most part of intrinsic dislocations, and the boundaries are, in general, narrower. The structure of the subgrain boundaries is analogous to both coincidence ledge [23, 24] and grain boundary dislocation models [25]. For example, in the grain boundary dislocation models, a subgrain boundary is formed when two crystals are misoriented slightly from one another producing a unit cell of the O-lattice [25] which is large compared to the crystal lattice. The crystal boundaries are formed by dislocation networks where the intersection of the boundary with the O-lattice cell

Figure 5 An overall view of the typical subgrain boundary microstructures observed in a sample forged at 590°C.

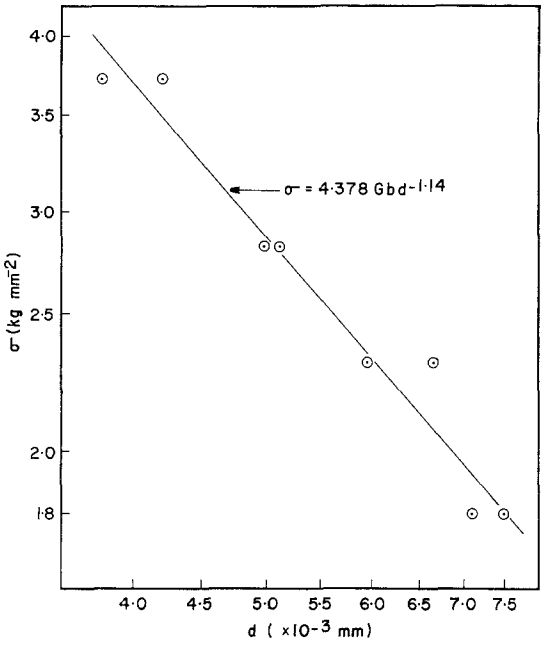

Figure 6 A graph of the approximate inverse relationship between flow stress, σ, and subgrain size, d, in hot-forged calcium fluoride. The line drawn through the data is a least-squares fit.

walls are the dislocation lines. The dislocation networks seen in Figs 1 to 4 range from 30 to 200 nm in size, which, in comparison to the lattice parameter of 0.546 nm, is large. Thus, the boundaries observed in hot-forged calcium fluoride are observed to show general agreement with subgrain boundary dislocation models.

The increase in subgrain boundary order with increasing temperature, reflected by a decrease in the extrinsic dislocation content has also been observed in other materials. In cold-rolled iron [26], as the temperature of deformation increases, the dislocation density decreases and the cell walls or subgrain boundaries become more ordered. A review of the results of the effect of temperature on the structure of cell walls formed in pure Cu and Al shows that raising the temperature of deformation produces a sharpening of cell walls, similar to the present results in calcium fluoride.

As in calcium fluoride, one of the first structural features that becomes evident during steady-state deformation of metallic or sodium chloride-type ionic materials is the appearance of subgrains. The size of subgrains in calcium fluoride is indirectly related to the temperature of deformation and is seen to increase with increasing temperature. Similar results are seen in Al [27, 28], Cu [29], Fe [1], sodium chloride [11], and potassium chloride [9].

The inverse dependence of flow stress on subgrain size in calcium fluoride has been predicted [1, 12, 30] and experimentally found to hold true in metallic systems [4], sodium chloride [9, 31], and potassium chloride [9]. Most importantly, the present work demonstrates that increases in the flow stress of calcium fluoride can be achieved through subgrain strengthening.

The dislocation tangles, networks and subgrain boundaries observed in hot-forged samples of calcium fluoride suggest that deformation is controlled by obstacle-limited glide of dislocations and/or power-law creep. Comparison of the stress ($4 \times 10^{-4} \leqslant \sigma/G \leqslant 9 \times 10^{-4}$), strain rate ($4 \times 10^{-2}\,\text{sec}^{-1}$) and temperature ($0.53 \leqslant T/T_m \leqslant 0.72$) ranges employed in the present hot-forging experiments of calcium fluoride with deformation maps constructed for sodium chloride and lithium fluoride [32] lends support to these mechanisms. Dislocation densities measured from the subgrain boundaries and interiors, as well as the total dislocation density could not be correlated to the measured flow stress in a manner totally consistent with forest mechanisms of work hardening. The total dislocation density was measured to decrease, as expected from forest models of hardening, with decreasing flow stress. However, the average spacing of dislocations in the subgrain boundaries was found to decrease with decreasing flow stress. Assuming, as in forest models, the stress to overcome an obstacle is inversely proportional to the obstacle spacing, the observed decrease of the dislocation spacing in the subgrain boundaries with decreasing stress (higher forging temperatures) is in direct conflict with such models. Therefore, a forest mechanism of hardening cannot solely account for the observed behaviour. Also, the higher forging temperatures, by providing an increased thermal activation, probably reduce the effectiveness of the subgrain boundaries as obstacles to dislocation motion. Above $0.5\,T_m$ dislocations are able to climb as well as glide. If a dislocation encounters an obstacle, climb may release it, allowing it to glide to the next obstacle, where the process may be repeated. While the glide step is responsible for almost all the strain, the average velocity of the dislocation will be determined by the climb step. The important feature of this mechanism of flow is that the rate-controlling process, at an atomic level, is the diffusion of

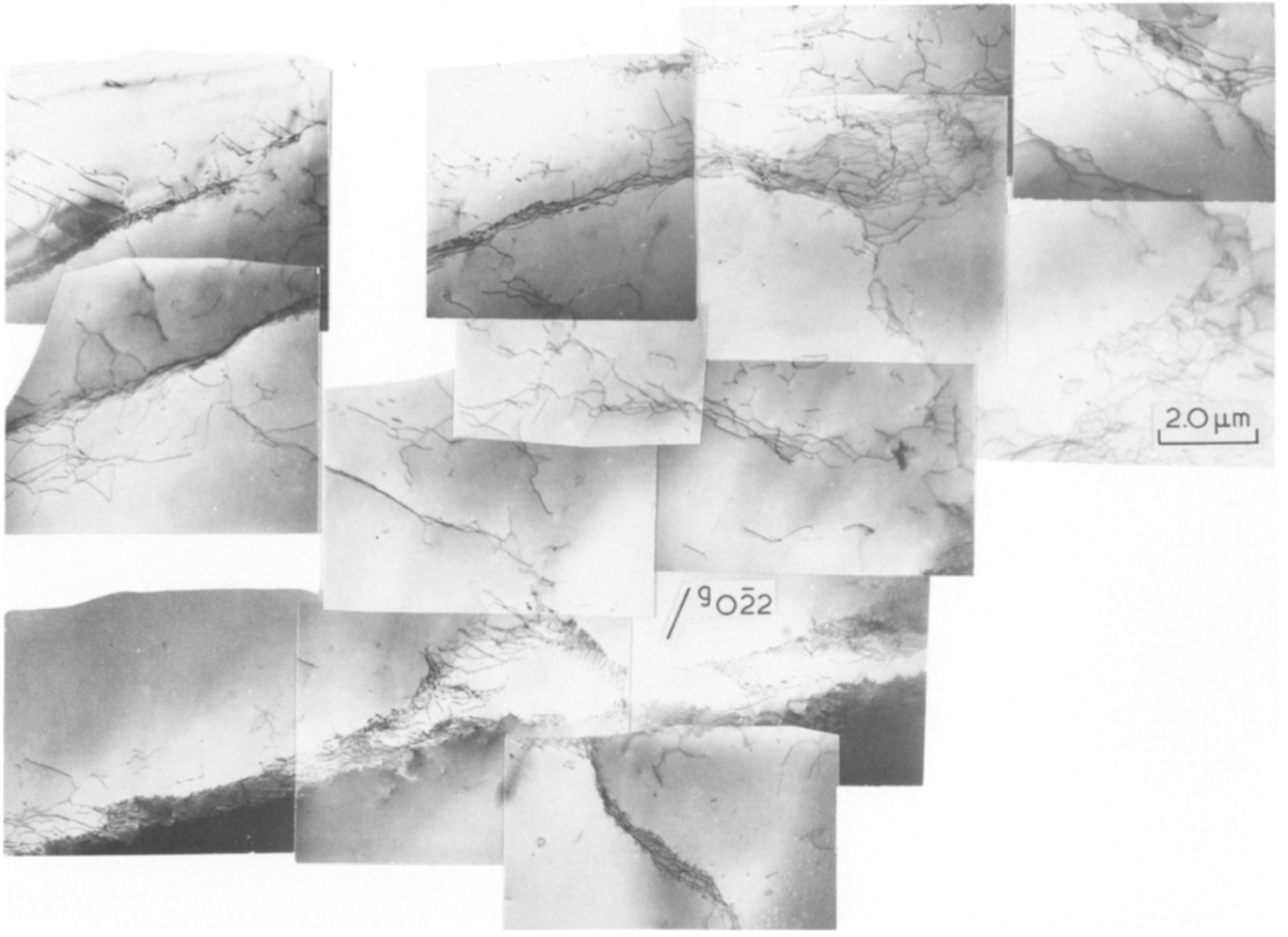

Figure 7 A TEM montage of a section of a sample forged at 590° C containing a non-uniform distribution of subgrain sizes and a wide variation in subgrain boundary complexity.

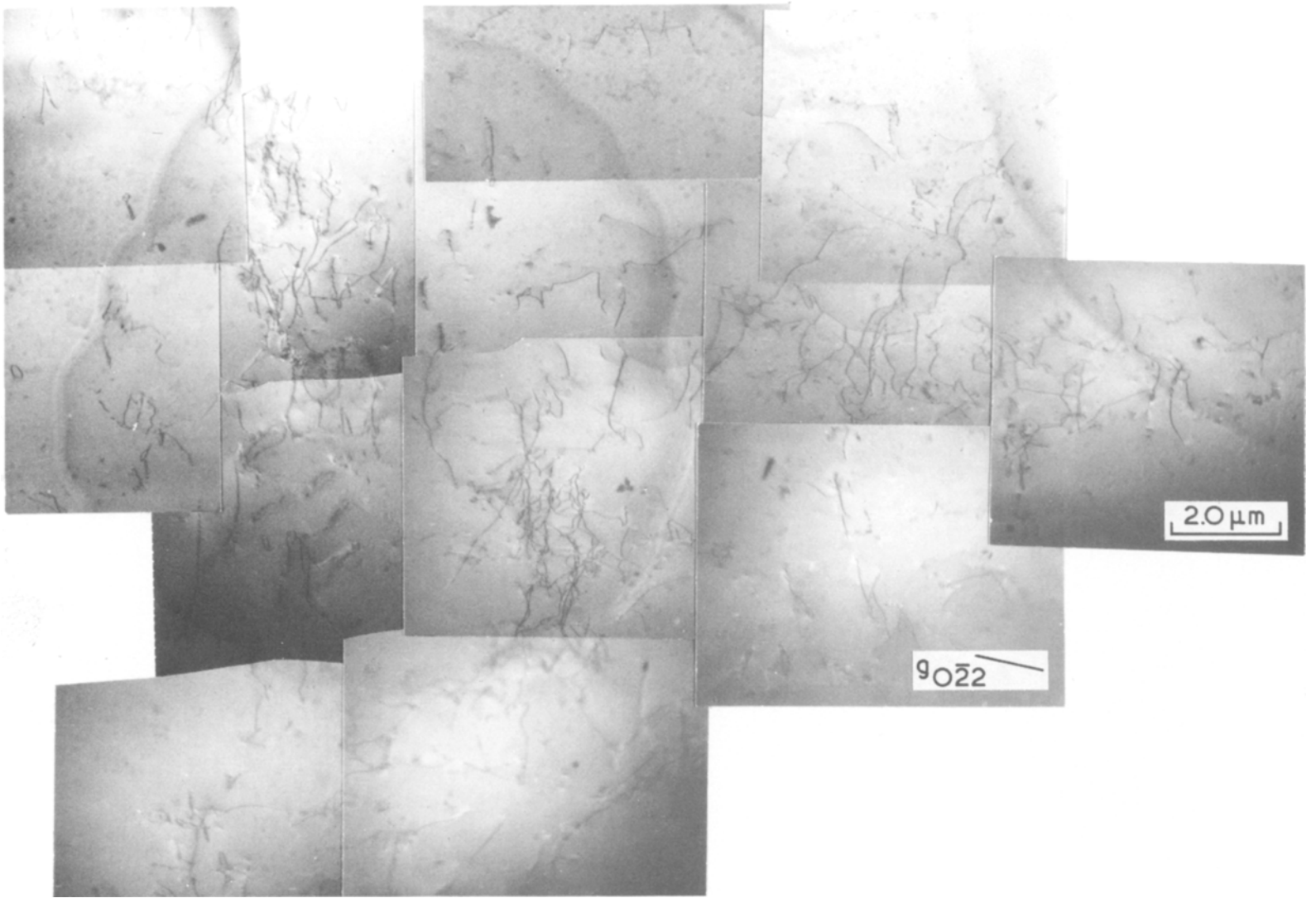

Figure 8 A TEM montage of a section of a sample forged at 907° C. Note the absence of subgrain boundaries and a well developed microstructure.

single ions or vacancies to or from the climbing dislocation, rather than the activation of dislocation glide itself. Thus, power-law creep should play an increasingly important role in the deformation behaviour with increasing temperature.

Hot-forging experiments of calcium fluoride were performed at conditions of steady-state deformation, where simultaneous work hardening and recovery processes determine the nature of the deformation microstructures. While at any one point in time local fluctuations may give rise to the formation of a subgrain-free region, the concurrent deformation will restore the microstructure. The non-uniform microstructures presented in Figs 7 (590° C) and 8 (907° C) were not, in general, characteristic of the overall microstructure. Regions such as those presented in Figs 7 and 8 may have two possible origins. First, the high strains employed in the hot-forging experiments increase the influence of platten effects in producing non-homogeneous flow, where the actual local stress is different from the applied stress, thus resulting in a non-uniform microstructure [14]. Second, recrystallization and recovery may occur during deformation or while the sample is cooling to room temperature. The recovery processes involve the annihilation of dislocations in subgrain interiors, within subgrain boundaries and the accommodation of matrix dislocations into the subgrain boundaries. In general, these processes require both glide and climb and, therefore, are aided by thermal activation at higher temperatures [13, 14].

5. Conclusions

Hot-forging experiments of calcium fluoride single crystals have been performed to true strains, ϵ, between $\epsilon = 0.3$ and 0.50 at temperatures between 590 and 907° C. TEM has been successfully applied, with the aid of a double-tilt liquid-helium cold-stage to characterize the deformation microstructures. The microstructure has been seen to consist of cell walls or subgrain boundaries. The redundant dislocation density present in the subgrain boundaries decreases and the degree of order within the subgrain boundaries increases with increasing deformation temperature. Measurements have shown the flow stress to be inversely proportional to the subgrain size. For the given stress and temperature ranges, deformation is suggested to be controlled by obstacle-limited glide of dislocations and/or power-law creep. The observed regions of non-uniform microstructure are thought to arise from platten effects caused by the high strain levels, or recovery during cooling or after hot-forging. Despite these non-uniform regions, subgrain formation through hot-forging appears to be a viable means of improving the flow stress of calcium fluoride single crystals.

Acknowledgements

The authors gratefully acknowledge Professor R. M. Cannon and A. Glaeser for their support and many valuable comments on this work.

References

1. C. LANGFORD and M. COHEN, *Trans ASM* **62** (1969) 623.
2. J. E. PRATT, *Acta Metall.* **15** (1967) 319.
3. J. D. LIVINGSTON, *ibid.* **10** (1962) 229.
4. M. R. STAKER and D. L. HOLT, *ibid.* **20** (1972) 569.
5. J. E. BAILEY and P. B. HIRSCH, *Phil. Mag.* **5** (1960) 485.
6. C. E. FELTNER and C. LAIRD, *Acta Metall.* **15** (1967) 1633.
7. C. E. FELTNER, *ibid.* **11** (1963) 817.
8. S. A. KULIN, P. P. NESHE and K. KREDER, Technical Report, AFML-TR-74-17 Man Labs, Inc., Cambridge, Massachusetts (1974).
9. M. F. YAN, R. M. CANNON, H. K. BOWEN and R. L. COBLE, in "Deformation of Ceramic Materials", edited by R. E. Tressler and R. C. Brandt (Plenum Publishing Corporation, New York, 1975) p. 549.
10. B. G. KOEPKE, R. H. ANDERSON and R. J. STOKES, in "Deformation of Ceramic Materials", edited by R. E. Tressler and R. C. Brandt (Plenum Publishing Corporation, New York, 1975). p. 497.
11. G. STREB and B. REPPICH, *Phys. Stat. Sol. (a)* **1b** (1973) 492.
12. D. KUHLMANN-WILSDORF, *Metall. Trans.* **1** (1970) 3173.
13. R. M. CANNON, H. K. BOWEN, A. M. GLAESER, H. J. MAYSON, F. A. McCLINTOCK, W. M. SHERRY, J. B. VANDER SANDE and M. F. YAN, Proceedings of the Symposium on Laser-Induced Damage in Optical Materials, NBS Special Publication number 462 (National Bureau of Standards, Washington, 1976) p. 69.
14. R. R. TURK, in "Deformation of Ceramic Materials", edited by R. E. Tressler and R. C. Brandt (Plenum Publishing Corporation, New York, 1975) p. 531.
15. H. V. WINSTON, R. R. TURK, R. C. PASTOR and R. F. SCHOLL, Proceedings of the Fourth Annual Conference on Infra-red Laser Window Materials, Army Research Progress Administration, Tucson, Arizona (1975) p. 437.
16. J. FENTER and G. GRAVES, Proceedings of the Fifth Annual Conference on Infrared Laser Window Materials Meeting, Army Research Progress Administration, Boulder, Colorado (1976) p. 181.

17. R. H. ANDERSON, B. G. KOEPKE and E. G. BERNAL, Proceedings of the Symposium on Laser-Induced Damage in Optical Materials, (NBS Special Publication number 462 (National Bureau of Standards, Washington, 1976) p. 87.
18. R. HILL, "Plasticity" (Oxford University Press, London, 1950).
19. W. M. SHERRY and J. B. VANDER SANDE, *Phil. Mag.* **40**, 1 (1979) 77.
20. P. B. HIRSH, A. HOWIE, R. B. NICHOLSON, D. W. PASHLEY and M. J. WHELAN, "Electron Microscopy of Thin Crystals" (Butterworths, London, 1965).
21. E. E. UNDERWOOD, "Quantitative Stereology" (Addison-Wesley, Reading, Mass., 1975).
22. A. H. COTTRELL, "Dislocations and Plastic Flow in Crystals" (Clarendon Press, Oxford, 1965) p. 51.
23. H. GLEITER and B. CHALMERS, *Prog. Mat. Sci.* **16** (1972) 1.
24. G. H. BISHOP and B. CHALMERS, *Scripta Met.* **2** (1968) 133.
25. W. BOLLMANN, "Crystal Defects and Crystalline Interfaces" (Springer-Verlag, Berlin, 1970) p. 1.
26. A. S. KEH and S. WEISSMANN, in "Electron Microcopy and Strength of Crystals," edited by G. Thomas and J. Washburn (Wiley-Interscience, New York, 1963) p. 231.
27. P. R. SWANN, in "Electron Microscopy and Strength of Crystals", edited by G. Thomas and J. Washburn (Wiley-Interscience, New York, 1963) p. 131.
28. H. J. McQUEEN, *J. Met.* **20** (1968) 31.
29. J. E. BAILEY, *Phil. Mag.* **8** (1963) 223.
30. D. L. HOLT, *J. Appl. Phys.* **41** (1970) 3197.
31. J. P. POIERIER, *Phil. Mag.* **26** (1972) 713.
32. R. A. VORRALL, R. J. FIELDS and M. F. ASHBY, Deformation-Mechanism Maps for LiF and NaCl, Technical Report No. 1, Division of Engineering and Applied Physics, Harvard University, 1975.

Received 21 August and accepted 10 October 1980.